Weisz, Phys. Lett. 67B, 321 (1977). For reviews see M. Karowski, Freie Universität Berlin Report No. FUB-HEP 19/1977 (to be published). (Talk presented at the "International School of Subnuclear Physics", Erice, Italy, 1977); B. Berg, Freie Universität Berlin Report No. FUB-HEP 23/1977 (to be published). (Seminar talk contributed to the Banff conference on "Particles and Fields", Banff, Canada, 1977).

[3]A. B. Zamolodchikov and Aj. B. Zamolodchikov, Nucl. Phys. B133, 525 (1978).

[4]B. Berg, M. Karowski, V. Kurak, and P. H. Weisz, Nucl. Phys. B134, 125 (1978).

[5]R. Shankar and E. Witten, Phys. Rev. D 17, 2134 (1978).

[6]S. Ø. Aks, J. Math. Phys. 6, 516 (1964).

[7]S. Coleman and J. Mandula, Phys. Rev. 159, 1251 (1967).

[8]M. Lüscher, Nucl. Phys. B135, 1 (1978).

[9]G. Källén and J. Toll, J. Math. Phys. 6, 299 (1965).

[10]J. Ya. Aref'eva and V. E. Korepin, Pis'ma Zh. Eksp. Teor. Fiz. 20, 680 (1974) [JETP Lett. 20, 312 (1974)].

[11]B. Berg, Nuovo Cimento 41A, 58 (1977).

[12]J. F. Schonfeld, Nucl. Phys. 122B, 1 (1977).

[13]A. B. Zamolodchikov and Aj. B. Zamolodchikov, Institute for Theoretical and Experimental Physics, Moscow, Report No. ITEP-112, 1977 (to be published).

[14]P. H. Weisz, Nucl. Phys. B122, 1 (1977).

[15]B. Berg, M. Karowski, V. Kurak, and P. H. Weisz, to be published.

[16]B. Berg, to be published.

[17]D. B. Melrose, Nuovo Cimento 40A, 181 (1965).

[18]B. Peterson, J. Math. Phys. 6, 1955 (1965).

Analysis of Pion-Nucleon Scattering up to 10 GeV/c

Archibald W. Hendry[(a)]
Lawrence Berkeley Laboratory, University of California, Berkeley, California 94720, and Physics Department,[(b)] *Indiana University, Bloomington, Indiana 47401*
(Received 10 April 1978)

I have analyzed pion-nucleon elastic scattering data from 1.6 GeV/c up to 10 GeV/c. The analysis makes use of a physical impact-parameter picture as an intermediate step. Many of the resulting partial-wave amplitudes show structure in their Argand plots. These are discussed in terms of possible high-spin resonances.

This Letter reports the results of a detailed analysis of pion-nucleon scattering. The analysis was carried out over a wide range of energies, overlapping with previous analyses[1-4] at the lower end, but extending well beyond them up to 10 GeV/c. The aim of the investigation was to see whether there was any evidence for any new high-mass resonances. Such states are predicted by almost all present theories of hadronic states, either as members of Regge families or as higher excitations of constituents, but none so far has been seen. We find that the partial waves which emerge from this analysis do indeed show interesting resonancelike behavior. Assuming a resonance plus background approximation, I extract corresponding values of masses and widths. These values should be important for future comparison with theoretical models.

It should be understood that this analysis is not a complete reanalysis of pion-nucleon scattering going all the way up from threshold. Rather, the emphasis is on looking at data above the region which has been thoroughly analyzed before, in the hope of detecting the more prominent resonances, should any exist. I do, however, choose an overlap region ($p_{lab}=1.6$–2.74 GeV/c) so that this analysis can be compared with the other analyses there and at the same time provides a guideline for the extension to higher energies.

The actual laboratory momenta at which the analysis was carried out were 1.6, 1.8, 1.99, 2.19, 2.30, 2.39, 2.50, 2.74, 3.0, 3.5, 4.0, 5.0, 6.0, and 10.0 GeV/c. The data at the higher momenta are probably more plentiful than one might realize, though of course their total amount is small compared to the wealth of data in the more-investigated lower region. For the beam momenta mentioned above 2.74 GeV/c, there are $\pi^{\pm}p$ differential cross-section measurements over all or most of the angular range, with some polarizations near the forward and usually also the backward direction. There are less charge-exchange data, but for all momenta there are differential cross sections at least in the forward and backward directions, and polarizations in the forward direction. In addition, I take the amplitudes at $\theta=0°$ as given from forward dispersion relations.[5]

A study of the data indicates that much is happening in this higher-energy domain. It is true that the shapes of the differential cross sections and polarizations near the forward direction have more or less settled down (apart from some gradual shrinkage) to what are known to be their shapes all the way up to ~200 GeV (Fermilab energies). However, in the intermediate angle range, there are several deep valleys which develop and then go away as the energy increases. Also, I mention the oscillations in the $\pi^{\pm}p$ and charge-exchange differential cross sections at 180° that have been known for some time. Perhaps strangest of all is the polarization in the vicinity of the backward direction (the polarization of course vanishes identically at 180°), which at first sight seems to fluctuate rather wildly as the energy is changed. I have tried to keep these experimental features in mind as I performed the analysis since part of my aim was to understand how these features came about from the contributing partial waves.

This analysis also has a new approach, in the sense that I did not follow the canonical way of many partial-wave analyses, which usually is to parametrize the individual phase shifts $\delta_{l\pm}$ and inelasticities $\eta_{l\pm}$ for each orbital angular momentum and isospin. This way becomes less practical as the number of partial waves that have to be included increases (at 10 GeV/c, partial waves up through at least $l=25$ have to be included). Instead, I chose to do the analysis in two steps.

The first step is to attempt to fit the data on the basis of a reasonable physical model. This model incorporates features that are generally believed to describe the general picture of hadronic scattering, namely, one in which much of the scattering can be understood in terms of a substantial diffraction component, together with a smaller contribution from peripheral scattering. To perform the first step therefore, I adopted an impact-parameter type of representation into which these features can be easily built. For example, we may write

$$\mathrm{Im}(kf_l) = Ae^{-Bb^2} + [D + (-1)^{l+1}E]e^{-C(b-r)^2}, \qquad (1)$$

where $b = l/k$. A sum over l is retained in the full amplitude, not an integral over b. The two parts on the right-hand side of (1) have a clear physical interpretation. Actually this is a tremendous advantage since one can quickly develop a feeling for appropriate values of the parameters. For instance, A and B in (1) above are determined essentially by the size and slope of the forward diffraction peaks in elastic $\pi^{\pm}p$ scattering, while r is approximately 1 fm for both. With a little thought, good guesses can be made for many of the parameters. Moreover, these b-space parameters do not change much from energy to energy (even though the individual l partial waves change), which is clearly advantageous for continuity and stability.

The main hope of this first step is that it will provide values of the real and imaginary parts of $kf_{l\pm}(I=\frac{3}{2}$ and $\frac{1}{2})$ which are fairly close to the correct ones. This will be true if our physical picture of diffraction plus peripheral scattering is a good one. The second step in our analysis was therefore to let the individual partial waves vary freely around their values determined in the first step, but the final values of the partial waves were never far from the values obtained in Step 1. The solution seems to be a stable one, though I did not search everywhere in partial-wave amplitude space to check on the possibility of others.

This two-step procedure was tested over the lower-momentum range 1.6–2.74 GeV/c, and the resulting partial-wave amplitudes compared with the Saclay values.[1,6] The agreement was very reasonable (since I incorporated data that have only recently become available, perfect agreement was not expected).

Fortified by these lower-energy fits, I proceeded to the higher energies. This is where the strength of the method becomes clearer. For the same number of parameters $A, B, \ldots$, we can include as many partial waves as are necessary in Step 1. It is only in Step 2 that a large number of parameters need to be varying simultaneously. (Perhaps my approach may be practical in analyzing other scattering processes when one proceeds to higher energies and where the quality of the data is deteriorating; compared to standard methods, my procedure is quick and can be done with only moderate computing facilities.)

The final product of an analysis of this kind is a long table of partial-wave amplitudes and many Argand diagrams. A report with full details of all the amplitudes is in preparation. Here I illustrate my results with a few Argand diagrams. Figure 1 shows the partial-wave behavior for the $f_{l\pm}(I=\frac{3}{2})$ waves $H_{3,11}$, $K_{3,15}$, and $M_{3,19}$; the $f_{l-}(I=\frac{3}{2})$ waves $G_{3,7}$, $H_{3,9}$, and $I_{3,11}$; the $f_{l+}(I=\frac{1}{2})$ waves $G_{1,9}$ and $I_{1,13}$; and the $f_{l-}(I=\frac{1}{2})$ waves $H_{1,9}$, $I_{1,11}$, $K_{1,13}$, and $M_{1,17}$. Most of these clearly show resonancelike loops. For the higher partial waves, the Argand diagrams are essentially of two types. The $f_{l+}(I=\frac{3}{2})$ and $f_{l-}(I=\frac{1}{2})$ amplitudes typically

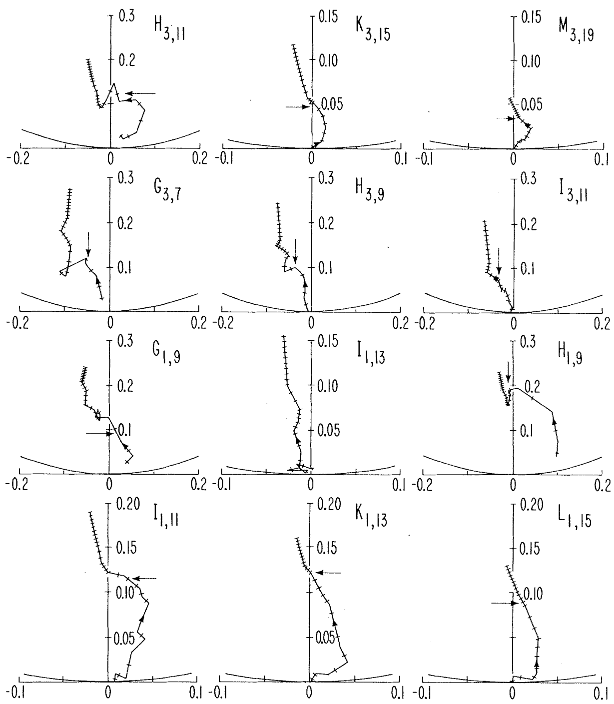

FIG. 1. Argand diagrams for a selection of partial waves. Cross marks occur at intervals of 50 MeV. The resonance positions corresponding to the values in Table I are indicated by the separate arrows.

TABLE I. Resonance parameters.

		Mass (GeV) $M \pm \Delta M$		Full Width(GeV) $\Gamma \pm \Delta\Gamma$		Elasticity $x \pm \Delta x$	
$f^{3/2}_{\ell+}$	G_{39}	2.20	0.10	0.45	0.20	0.10	0.03
	$H_{3,11}$	2.40	0.06	0.46	0.10	0.11	0.02
	$I_{3,13}$	2.65	0.10	0.50	0.10	0.05	0.01
	$K_{3,15}$	2.85	0.10	0.70	0.20	0.03	0.01
	$L_{3,17}$	3.30	0.20	1.10	0.30	0.03	0.01
	$M_{3,19}$	3.70	0.20	1.30	0.40	0.025	0.01
	$N_{3,21}$	4.1	0.3	1.6	0.5	0.018	0.01
$f^{3/2}_{\ell-}$	G_{37}	2.28	0.08	0.40	0.15	0.09	0.02
	H_{39}	2.45	0.10	0.50	0.20	0.08	0.02
	$I_{3,11}$	2.85	0.15	0.70	0.20	0.06	0.02
	$K_{3,13}$	3.2	0.2	1.0	0.3	0.045	0.02
$f^{1/2}_{\ell+}$	G_{19}	2.2	0.1	0.35	0.10	0.09	0.02
$f^{1/2}_{\ell-}$	G_{17}	2.14	0.04	0.27	0.05	0.16	0.04
	H_{19}	2.30	0.10	0.45	0.15	0.12	0.04
	$I_{1,11}$	2.70	0.10	0.90	0.10	0.08	0.02
	$K_{1,13}$	3.00	0.10	0.90	0.15	0.07	0.02
	$L_{1,15}$	3.50	0.20	1.3	0.2	0.055	0.02
	$M_{1,17}$	3.80	0.20	1.6	0.2	0.040	0.015
	$N_{1,19}$	4.1	0.2	1.9	0.3	0.030	0.015

first develop positive real parts, but then get overtaken by a slowly varying "background" (coming from the diffractive component in the particular partial wave; it has a growing negative real part and a growing positive imaginary part). This "background" component is stronger in the case of the $f_{l-}(I=\frac{3}{2})$ and $f_{l+}(I=\frac{1}{2})$ amplitudes so that the higher partial waves take off towards negative real values in the Argand diagrams. The latter waves show much less structure and less can be said about them.

It is a matter of dispute as to whether loops in Argand diagrams correspond to resonances or not. However, if they are interpreted as resonances, I obtain the values shown in Table I for their masses, widths, and elasticities. These numbers were deduced by assuming a Breit-Wigner shape multiplied by a phase factor, plus a smooth background. Generally speaking, however, the resonance parameters are determined by the first half of the resonance since the resonance quickly becomes submerged in the background as the energy increases. The ranges within which I believe the resonance parameters lie are also indicated in the table.

Plots of the resonance spins j against the mass M, the mass squared, and the pion-nucleon c.m. momentum k show that these resonances fall on effective linear trajectories of the form $j \sim kR$, with R about 1 fm. In a sense, this is not surprising since it is expected in various theoretical models. However, I stress that it is *necessitated by the data,* such as $\pi^{\pm}p$ crossover, the shape of $d\sigma(\pi^+p)/dt$ near the backward direction, etc. I also find that the peripheral partial waves play an important part in explaining some of the more subtle experimental features observed in the 1.6–10-GeV/c region. For example, the π^+p polarizations near the backward direction, which as mentioned earlier vary quite rapidly with energy, can be shown to arise[7] from alternate constructive and destructive interference between successive peripheral waves (which change sign with increasing l) and a slowly varying piece from the lower partial waves. I therefore expect my results to contain general features of other analyses over this energy region.

I would like to thank Charles R. Ellis for assistance in computing. I also wish to thank Professor G. Chew and Professor J. D. Jackson for the hospitality of the Lawrence Berkeley Laboratory. This work was supported in part by the U. S. Department of Energy.

[(a)]Participating Guest, Lawrence Berkeley Laboratory, University of California, Berkeley, Calif. 94720.
[(b)]Permanent address.

[1]R. Ayed and P. Bareyre, unpublished; T. G. Trippe *et al.*, Rev. Mod. Phys. 48, No. 2, Pt. 2, S51 (1976).
[2]R. E. Cutkosky, R. E. Hendrick, and R. L. Kelly, Phys. Rev. Lett. 37, 645 (1976).
[3]D. M. Chew and M. Urban, in *Proceedings of the Topical Conference on Baryon Resonances*, edited by R. T. Ross and D. H. Saxon (Oxford Univ. Press, Oxford, 1976), p. 156.
[4]E. Pietarinen, in *Proceedings of the Topical Conference on Baryon Resonances*, edited by R. T. Ross and D. H. Saxon (Oxford Univ. Press, Oxford, 1976), p. 20. This analysis is also being done up to 10 GeV/c.
[5]G. Höhler, H. P. Jakob, and R. Kaiser, Tables of Pion-Nucleon Forward Amplitudes, University of Karlsruhe, 1976 (unpublished); R. E. Hendrick and B. Lautrap, Phys. Rev. D 11, 529 (1975).
[6]I thank Dr. R. Kelly for forwarding the data of Ayed and Bareyre (Ref. 1) to us prior to publication.
[7]F. Halzen, M. G. Olsson, and A. Yokosawa, Nucl. Phys. B113, 269 (1970) have also suggested the importance of the peripheral waves for these data, based on the Saclay results (Ref. 1).

Inadequacy of the Coupled-Channels Born Approximation for Explaining Anomalous Rare-Earth (d,t) Transitions

J. C. Peng, H. S. Song, F. C. Wang, and J. V. Maher
University of Pittsburgh, Pittsburgh, Pennsylvania 15260
(Received 10 April 1978)

A CCBA (coupled-channels Born approximation) analysis is used to study the importance of multistep processes involving quadrupole inelastic excitations in producing anomalously shaped angular distributions for rare-earth (d,t) transitions. The CCBA results are compatible with DWBA (distorted-wave Born approximation) results in the cases where the DWBA works well and tend to improve agreement for the anomalous transitions —but the overall agreement is still rather poor and additional improvements in the reaction calculations will be needed to understand the anomalous transitions.

The importance of multistep reaction mechanisms is well established for several multinucleon transfer reactions, and coupled-channels Born-approximation (CCBA) analyses have been strikingly successful in explaining many such cases.[1] These successes of the CCBA approach have encouraged a belief that most, if not all, anomalously shaped angular distributions for single-nucleon-transfer reactions could also be explained with a CCBA approach. However, the CCBA analyses of single-nucleon-transfer reactions have been applied to restricted data sets and have concentrated[2] on (p,d) transitions [where significant changes of angular distribution shape can be effected even within a distorted-wave Born-approximation (DWBA) analysis by exploiting optical potential ambiguities. This strong sensitivity of (p,d) calculations to choice of optical-potential parameters presumably arises from the long mean free path of the proton in the nucleus; for analogous (d,t) transitions, where both projectile and ejectile are strongly absorbed in the nuclear interior, the DWBA predictions for angular distribution shapes are very stable against reasonable parameter variations.[3]] Until recently, very few complete angular distributions had been measured for single-nucleon-transfer reactions on rare-earth nuclei, and so the DWBA analysis was assumed valid and was routinely applied to individual spectra to provide information on single-particle states for these nuclei.[4] An extensive set of angular distributions[3,5-7] has now become available for (d,t) transitions on ^{160}Gd, ^{162,164}Dy, and ^{166,168}Er. These angular distributions have shown that most of the (d,t) transitions are well described by DWBA calculations. However, a significant number of levels have angular distributions which either can only be fitted by DWBA calculations assuming orbital angular momentum transfer (l) values which are